Acta Crystallographica Section F
Structural Biology and Crystallization Communications
ISSN 1744-3091

Eiji Inagaki, Hitomi Takahashi, Chizu Kuroishi and Tahir H. Tahirov*

Advanced Protein Crystallography Research Group, RIKEN Harima Institute, 1-1-1 Kouto, Mikazuki-cho, Sayo-gun, Hyogo 679-5148, Japan

Correspondence e-mail: tahir@spring8.or.jp

Received 11 May 2005
Accepted 20 May 2005
Online 1 June 2005

Crystallization and avoiding the problem of hemihedral twinning in crystals of Δ^1-pyrroline-5-carboxylate dehydrogenase from *Thermus thermophilus*

Δ^1-Pyrroline-5-carboxylate dehydrogenase from *Thermus thermophilus* (*Tt*P5CDh) has been crystallized in a citrate-bound form (*Tt*P5CDh-cit). The crystals diffracted to well beyond 2 Å resolution, but exhibited perfect or near-perfect hemihedral twinning. Variation of crystallization conditions resulted in the growth of larger untwinned crystals or crystals with significantly reduced twin content, all with similar unit-cell parameters. The soaking of *Tt*P5CDh-cit crystals in citrate-free solution produced crystals of the apo form (*Tt*P5CDh-apo). The *Tt*P5CDh-apo crystals belong to space group *R*3, with unit-cell parameters $a = b = 102.29$, $c = 279.28$ Å, and diffract to 1.08 Å. Crystals soaked in solution with NAD^+ (*Tt*P5CDh-NAD), NADH (*Tt*P5CDh-NADH) and glutamate (*Tt*P5CDh-Glu) were also prepared and characterized.

1. Introduction

Δ^1-Pyrroline-5-carboxylate (P5C) or glutamate-γ-semialdehyde (GSA, uncyclized tautomer in spontaneous equilibrium with P5C) is the common intermediate in amino-acid metabolic pathways involving interconversions of glutamate, ornithine and proline (Phang *et al.*, 2001). P5C dehydrogenase (P5CDh; EC 1.5.1.12) catalyzes the irreversible oxidation of GSA into glutamate, with the reduction of NAD^+ to NADH. In humans, P5C is both the intermediate precursor and the degradation product of proline (Phang *et al.*, 2001). Two inherited disorders of the proline metabolic system result in hyperprolinaemia. Type II hyperprolinaemia (HPII) arises from a deficiency of P5CDh (Valle *et al.*, 1974) and proline levels in plasma are elevated tenfold to 15-fold (Phang *et al.*, 2001).

From analysis of amino-acid sequence, P5CDh was reported to belong to the superfamily of aldehyde dehydrogenases (ALDhs; Sophos & Vasiliou, 2003). The protein structures of several members of the ALDh superfamily have been reported, including the class 1–3 and 9 ALDhs (Moore *et al.*, 1998; Steinmetz *et al.*, 1997; Liu *et al.*, 1997; Johansson *et al.*, 1998) and non-phosphorylating glyceraldehyde-3-phosphate dehydrogenase (Cobessi *et al.*, 1999). These structures adopt the same basic fold and exist in a dimeric or tetrameric state (or dimer of dimers).

The genome sequence of *Thermus thermophilus* HB8 contains a gene *TT0033* encoding a protein that shares 48 and 31% sequence identity with the monofunctional P5CDhs rocA of *Bacillus subtilis* and human put2, respectively (Glaser *et al.*, 1993; Hu *et al.*, 1996). In order to resolve the catalytic mechanism, P5CDh structures are required in both the apo form and ligand-bound forms. Here, we report the crystallization and preliminary crystallographic studies of the product of *T. thermophilus* gene *TT0033* (*Tt*P5CDh) in a citrate-bound form (*Tt*P5CDh-cit). Crystals of *Tt*P5CDh in the apo form (*Tt*P5CDh-apo), in the NAD^+-bound form (*Tt*P5CDh-NAD), in the NADH-bound form (*Tt*P5CDh-NADH) and in the glutamate-bound form (*Tt*P5CDh-Glu) were also prepared and characterized.

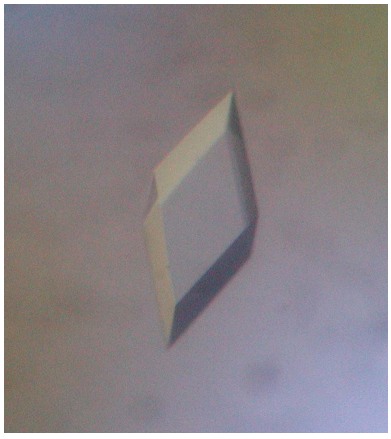

2. Materials and methods

2.1. Expression and purification

The protocols used for the expression and purification of *Tt*P5CDh were similar to those described for phosphopantetheine adenylyl-

Table 1
Crystal parameters and data-collection statistics.

Values in parentheses are for the outer shell.

Crystal	*Tt*P5CDh-apo	*Tt*P5CDh-NAD	*Tt*P5CDh-NADH	*Tt*P5CDh-Glu	*Tt*P5CDh-cit	
					Untwinned	Twinned
Crystal parameters						
Unit-cell parameters (Å)						
a	102.29	102.18	102.01	102.62	102.19	102.09
c	279.28	278.61	278.32	279.07	279.36	279.53
Space group	*R*3	*R*3	*R*3	*R*3	*R*3	*R*3
Z	18	18	18	18	18	18
Solvent content (%)	50.1	49.9	50.0	50.4	50.0	50.0
Data collection						
Temperature (K)	100	100	100	100	100	100
X-ray source	BL26B1	BL26B1	BL26B1	BL26B1	BL45PX	Rigaku FR-D
Detector	R-AXIS V	R-AXIS V	R-AXIS V	R-AXIS V	R-AXIS V	R-AXIS IV
Wavelength (Å)	0.8	0.8	1.0	0.8	1.02	1.542
Resolution (Å)	30–1.08 (1.10–1.08)	50–1.8 (1.83–1.80)	40–1.9 (1.94–1.90)	30–1.3 (1.32–1.30)	50–1.35 (1.37–1.35)	50–1.9 (1.97–1.90)
Unique reflections	450606	99097	85240	255946	232992	83382
Redundancy	3.1 (2.3)	3.7 (3.7)	4.0 (3.0)	2.8 (2.2)	3.5 (3.2)	2.6 (1.7)
Completeness (%)	96.3 (91.4)	98.4 (99.9)	100.0 (100.0)	95.0 (90.2)	97.8 (95.5)	97.3 (84.3)
$R_{\rm merge}$	6.3 (51.3)	11.3 (54.0)	7.8 (46.0)	7.5 (42.1)	6.3 (27.2)	6.7 (17.3)
$\langle I/\sigma(I)\rangle$	21.6 (2.0)	14.1 (3.4)	17.3 (2.2)	11.5 (2.0)	35.0 (5.4)	17.4(4.3)
Twin fraction†						
$(h, -h - k, -l)$	0.173	0.018	0.093	0.020	0.061	0.385
$(h + k, -k, -l)$	0.070	0.013	0.043	0.014	0.041	0.123
$(-h, -k, -l)$	0.081	0.020	0.060	0.023	0.049	0.128

† Twin fractions (Yeates, 1997) for possible twinning operators in space group *R*3 were calculated using the detect_twinning.inp protocol implemented in *CNS* (Brünger *et al.*, 1998).

transferase by Takahashi *et al.* (2004). Briefly, the gene was amplified by the polymerase chain reaction (PCR) using *T. thermophilus* HB8 genomic DNA as the template. The PCR product was ligated with pT7blue (Novagen). The plasmid was digested with *Nde*I and *Bgl*II and the fragment was inserted into the expression vector pET-11a linearized with *Nde*I and *Bam*HI. The cells were suspended in 20 m*M* Tris–HCl pH 8.0 (buffer *A*) containing 0.5 *M* NaCl and 5 m*M* 2-mercaptoethanol and disrupted by sonication. The supernatant was heated at 343 K for 13 min. After heat treatment, the cell debris and denatured proteins were removed by centrifugation (15000 rev min^{-1}, 30 min) and the supernatant solution was used as the crude extract for purification. The crude extract was desalted using a HiPrep 26/10 desalting column (Amersham Biosciences) and loaded onto a SuperQ Toyopearl 650M column (Tosoh) equilibrated with buffer *A*. The protein was eluted with a linear gradient of 0–0.3 *M* NaCl. The fraction containing the protein was desalted with HiPrep 26/10 with buffer *A* and subjected to a Resource Q column (Amersham Biosciences) equilibrated with buffer *A*. The protein was eluted with a linear gradient of 0–0.3 *M* NaCl. The fraction containing the protein was desalted with HiPrep 26/10 containing 10 m*M* phosphate pH 7.0 and applied onto a Bio-Scale CHT-20-I column (Bio-Rad) equilibrated with the same buffer. The protein was eluted with a linear gradient of 10–150 m*M* phosphate pH 7.0. The main protein peak was desalted using a HiPrep 26/10 column with 50 m*M* sodium phosphate pH 7.0, after which ammonium sulfate was added to 0.9 *M*. The solution was loaded onto a Resource Phe1 (Amersham Biosciences) column equilibrated in the same buffer containing 0.9 *M* ammonium sulfate. The protein was eluted with a linear gradient of 0–0.9 *M* ammonium sulfate. The fractions containing the protein were pooled, concentrated by ultrafiltration (Amicon, 30 kDa cutoff) and loaded onto a HiLoad 16/60 Superdex 75 column (Amersham Biosciences) equilibrated with buffer *A* containing 50 m*M* NaCl. The purified protein was homogeneous on SDS–PAGE.

2.2. Crystallization

The initial crystallization conditions were obtained by the micro-batch method (Chayen *et al.*, 1990) using a 'TERA' crystallization robot and a screening kit designed for high-throughput protein crystallization (Sugahara & Miyano, 2002). A 0.5 µl aliquot of the screening solution was mixed with 0.5 µl protein solution containing 20 mg ml^{-1} protein, covered with 15 µl of a silicone and paraffin oil mixture and then kept at a temperature of 291 K. Many small diffraction-quality rhombohedral crystals appeared after one month from the screening solution containing 44% 2-methyl-2,4-pentanediol (MPD), 0.5 *M* lithium chloride and 0.1 *M* sodium citrate buffer pH 5.2. They all exhibited perfect or near-perfect hemihedral twinning.

In order to improve the size and quality of crystals and eliminate hemihedral twinning, further optimization of conditions was performed using the sitting-drop vapour-diffusion method. Drops of 1.5 µl 10 mg ml^{-1} protein solution with 1.5 µl reservoir solution were equilibrated against 500 µl reservoir solution at a temperature of 298 K in 24-well plates. Variations of initial conditions, including concentrations of components, pH and temperature, improved the

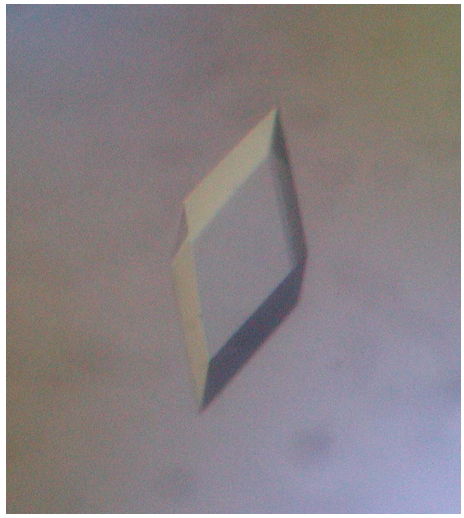

Figure 1
Photomicrograph of a *Tt*P5CDh-cit crystal.

Table 2
Intensity statistics for *Tt*P5CDh-cit crystal.

$\langle|I|^2\rangle/\langle|I|\rangle^2$ is 2.0 for untwinned data and 1.5 for twinned data. $\langle|F|\rangle^2/\langle|F|^2\rangle$ is 0.785 for untwinned data and 0.865 for twinned data. The statistics were calculated using *CNS* (Brünger *et al.*, 1998).

	*Tt*P5CDh-cit (twinned)		*Tt*P5CDh-cit (untwinned)	
Resolution (Å)	$\langle|I|^2\rangle/\langle|I|\rangle^2$	$\langle|F|\rangle^2/\langle|F|^2\rangle$	$\langle|I|^2\rangle/\langle|I|\rangle^2$	$\langle|F|\rangle^2/\langle|F|^2\rangle$
5.43–50.0	1.8131	0.8423	1.9638	0.8107
4.31–5.43	1.6362	0.8617	1.8265	0.8232
3.76–4.31	1.5653	0.8713	1.7865	0.8314
3.42–3.76	1.6170	0.8655	1.7790	0.8330
3.17–3.42	1.6193	0.8675	1.7839	0.8296
2.99–3.17	1.6017	0.8682	1.8266	0.8236
2.84–2.99	1.5690	0.8720	1.7914	0.8254
2.71–2.84	1.5855	0.8707	1.8216	0.8224
2.61–2.71	1.5825	0.8698	1.8205	0.8208
2.52–-2.61	1.6231	0.8725	1.8367	0.8166
2.44–2.52	1.7160	0.8595	1.9586	0.8106
2.37–2.44	1.6366	0.8686	1.8981	0.8142
2.31–2.37	1.5528	0.8767	1.8792	0.8142
2.25–2.31	1.5936	0.8720	1.9337	0.8102
2.20–2.25	1.5503	0.8769	1.8613	0.8168
2.15–2.20	1.5804	0.8732	1.9688	0.8067
2.11–2.15	1.5177	0.8806	1.8603	0.8182
2.07–2.11	1.5457	0.8817	1.8118	0.8218
2.03–2.07	1.5535	0.8773	1.9361	0.8097
2.00–2.03	1.5398	0.8788	1.9143	0.8119
Average	1.6001	0.8703	1.8628	0.8186

size and quality of the crystals; however, the problem of twinning persisted. Surprisingly, complete removal of lithium chloride produced crystals mainly without twinning, but occasionally some crystals appeared with partial hemihedral twinning. The best crystals of rhombohedral shape (Fig. 1) grew to dimensions of 0.3 × 0.2 × 0.2 mm in one week using reservoir solution containing 32% MPD and 50 m*M* sodium citrate buffer pH 5.2. Structural analysis of a crystal showed the presence of a citrate molecule in the substrate-binding site (Inagaki & Tahirov, unpublished results).

2.3. Removal and addition of ligands

The citrate was removed from the active site by soaking for 1 h in reservoir solution containing sodium acetate buffer instead of sodium citrate. The removal of bound citrate was confirmed by structural analysis (Inagaki & Tahirov, unpublished results). The obtained citrate-free crystals (*Tt*P5CDh-apo) were used for the preparation of ligand-bound forms by 2 h soaking in reservoir solution with the addition of 5 m*M* NAD^+ (*Tt*P5CDh-NAD), 5 m*M* NADH (*Tt*P5CDh-NADH) or saturated sodium glutamate (*Tt*P5CDh-Glu).

2.4. Data collection

For data collection, the crystals were mounted in nylon-fibre loops and flash-cooled in a dry nitrogen stream at 100 K. Complete diffraction data sets were collected from untwinned crystals at 100 K using synchrotron radiation at SPring-8 beamline BL26B1 or BL45PX. The data set from a twinned crystal of *Tt*P5CDh-cit was collected using Cu $K\alpha$ radiation from a Rigaku FR-D generator. All intensity data were indexed, integrated and scaled with *DENZO* and *SCALEPACK* implemented in the *HKL*2000 program package (Otwinowski, 1993; Otwinowski & Minor, 1997). The crystal parameters and data-processing statistics are summarized in Table 1.

3. Results and discussion

Calculation of the twin fraction (Yeates, 1997) with *CNS* (Brünger *et al.*, 1998) revealed the presence of perfect or near-perfect hemihedral twinning in all crystals grown from the lithium chloride-containing solutions. Perfect hemihedral twinning causes serious problems during phasing and refinement (Chandra *et al.*, 1999). It is very interesting that it was possible to obtain *Tt*P5CDh-cit crystals with similar unit-cell parameters but without hemihedral twinning after the exclusion of lithium chloride from the crystallization solution (Table 2).

Near-complete diffraction data sets were collected using one twinned and five untwinned crystals (Table 1). The diffraction resolutions were high for *Tt*P5CDh-cit, *Tt*P5CDh-apo and *Tt*P5CDh-Glu crystals at 1.35, 1.08 and 1.3 Å, respectively. Soaking with the cofactors NAD^+ and NADH reduced the overall crystal quality and the diffraction resolution fell to 1.8 and 1.9 Å, respectively. Solvent-content calculations (Matthews, 1968) suggested the presence of two *Tt*P5CDh subunits in the asymmetric unit, with a solvent content of 50% (Table 1). The *Tt*P5CDh-cit structure was solved by the molecular-replacement method using the coordinates of the retinal dehydrogenase type II monomer structure (PDB code 1bi9; Lamb & Newcomer, 1999) as a search model. The details of structure determination and refinement will be reported elsewhere.

We are grateful to Shigeyuki Yokoyama and Seiki Kuramitsu for the plasmid vector and Mitsuaki Sugahara for management of the automated crystallization. This work was supported by the National Project on Protein Structural and Functional Analysis funded by MEXT of Japan (Project TT0033/APCG00120).

References

Brünger, A. T., Adams, P. D., Clore, G. M., DeLano, W. L., Gros, P., Grosse-Kunstleve, R. W., Jiang, J.-S., Kuszewski, J., Nilges, M., Pannu, N. S., Read, R. J., Rice, L. M., Simonson, T. & Warren, G. L. (1998). *Acta Cryst.* D**54**, 905–921.
Chandra, N., Acharya, K. R. & Moody, P. C. (1999). *Acta Cryst.* D**55**, 1750–1758.
Chayen, N. E., Shaw Stewart, P. D., Maeder, D. L. & Blow, D. M. (1990). *J. Appl. Cryst.* **23**, 297–302.
Cobessi, D., Tete-Favier, F., Marchal, S., Azza, S., Branlant, G. & Aubry, A. (1999). *J. Mol. Biol.* **290**, 161–173.
Glaser, P., Kunst, F., Arnaud, M., Coudart, M. P., Gonzales, W., Hullo, M.-F., Ionescu, M., Lubochinsky, B., Marcelino, L., Moszer, I., Presecan, E., Rapoport, G. & Danchin, A. (1993). *Mol. Microbiol.* **10**, 371–384.
Hu, C. A., Lin, W. & Valle, D. (1996). *J. Biol. Chem.* **271**, 9795–9800.
Johansson, K., El-Ahmad, M., Ramaswamy, S., Hjelmqvist, L., Jornvall, H. & Eklund, H. (1998). *Protein Sci.* **7**, 2106–2117.
Lamb, A. L. & Newcomer, M. E. (1999). *Biochemistry*, **38**, 6003–6011.
Liu, Z.-J., Sun, Y. J., Rose, J., Chung, Y. J., Hsiao, C. D., Chang, W. R., Kuo, I., Perozich, J., Lindahl, R., Hempel, J. & Wang, B.-C. (1997). *Nature Struct. Biol.* **4**, 317–326.
Matthews, B. W. (1968). *J. Mol. Biol.* **33**, 491–497.
Moore, S. A., Baker, H. M., Blythe, T. J., Kitson, K. E., Kitson, T. M. & Baker, E. N. (1998). *Structure*, **6**, 1541–1551.
Otwinowski, Z. (1993). *Proceedings of the CCP4 Study Weekend. Data Collection and Processing*, edited by L. Sawyer, N. Isaacs & S. Bailey, pp. 56–62. Warrington: Daresbury Laboratory.
Otwinowski, Z. & Minor, W. (1997). *Methods Enzymol.* **276**, 307–326.
Phang, J. M., Hu, C. A. & Valle, D. (2001). *The Metabolic and Molecular Bases of Inherited Disease*, 8th ed., edited by C. R. Scriver, A. L. Beaudet, W. S. Sly & D. Valle, pp. 1821–1838. New York: McGraw–Hill.
Sophos, N. A. & Vasiliou, V. (2003). *Chem. Biol. Interact.* **143–144**, 5–22.
Steinmetz, C. G., Xie, P., Weiner, H. & Hurley, T. D. (1997). *Structure*, **5**, 701–711.
Sugahara, M. & Miyano, M. (2002). *Tanpakushitsu Kakusan Koso*, **47**, 1026–1032.
Takahashi, H., Inagaki, E., Fujimoto, Y., Kuroishi, C., Arisaka, F., Yutani, K., Kuramitsu, S., Yokoyama, S., Miyano, M. & Tahirov, T. H. (2004). *Acta Cryst.* D**60**, 97–104.
Valle, D., Goodman, S. I., Applegarth, D. A., Shih, V. E. & Phang, J. M. (1974). *J. Clin. Invest.* **58**, 598–603.
Yeates, T. O. (1997). *Methods Enzymol.* **276**, 344–358.